

Document-ID: 431337

Patron:

Note:

NOTICE:

Pages: 15 Printed: 05-09-04 16:54:48

Sender: Ariel/Windows

Texas A&M University Campus Libraries
Courier



ILLiad TN: 431337

Journal Title: Journal of Computational
Physics

Volume: 95

Issue: 1

Month/Year: 1991

Pages: 436-449

Article Author: Prabir Daripa

Article Title: Solvability Condition and its
Application to Fast Numerical Solution of
Overposed Problems in Compressible Flows

Call #: QC20.J64

Location: evans

Not Wanted Date: 11/03/2004

Status: Faculty

Phone: (979) 845 1204

E-mail: daripa@math.tamu.edu

Name: Prabir Daripa

Pickup at Evans

Address:

Ms-3368

College Station, TX 77843

Solvability Condition and Its Application to Fast Numerical Solution of Overposed Inverse Problems in Compressible Flows

PRABIR DARIPA

Department of Mathematics,
Texas A&M University, College Station, Texas 77843

Received June 26, 1989; revised April 2, 1990

In this paper we derive some results that give the existence of solutions (restricted by a compatibility condition) to overposed inverse design problems in a satisfactory manner. An overposed inverse design problem is concerned with generating a profile which will have a specified speed distribution $q_0^s(s)$ at a given free stream Mach number M_∞^s . This is equivalent to specifying pressure distribution. This problem has been of interest in aeronautical engineering. The overposedness of this problem is due to the specification of M_∞^s . An important issue has been the relation between $q_0^s(s)$ and M_∞^s . We derive this relation. A very useful approximation to this relation is established through numerical experiments which is exact for all practical purposes. We show the importance of this result in solving the overposed problem in an efficient manner. © 1991 Academic Press, Inc.

1. INTRODUCTION

Inverse problems have been addressed before in [1-4] with interesting new ideas. Basically there are two types of inverse design problems: well-posed and overposed. A well-posed inverse problem is concerned with the generation of a body which will have a specified speed distribution. An overposed inverse problem is concerned with the generation of a body which will have a specified speed distribution at a specified free stream Mach number. The overposedness is due to the specification of the free stream Mach number. An overposed problem has a solution only if the free stream Mach number is compatible with the specified speed distribution. This compatibility is decided by the equations of motion. Usually the compressible fluid flow equations are solved completely to determine the compatibility and hence the existence of a solution to the overposed problem is determined a posteriori.

In aeronautical engineering one often modifies a known pressure distribution C_p (we use the term pressure for pressure coefficient) over an airfoil in order to improve the performance of the airfoil which will have this modified C_p . Both, the free stream Mach number M_∞^s and the speed distribution q_0^s can be calculated from any arbitrary C_p without using the equations of motion. This is described in Section 2.10 of Ref. [5]. All flow variables in this paper refer to their values normalized

by their sonic value. We mean normalizing we mean normalizing. For example, below the supersonic subscript "o" to (Occasionally subscript context). Because the speed distribution modified C_p is over aeronautical consideration.

The central idea preferably no, not work with the equation has been shown to pose as shown in compressible fluid flow of the well-posed of the Beltrami function to the solution of mean value relation application of the M_∞^s and q_0^s which (iii) the application the overposed problem equations.

The rest of the of the Beltrami equation in Section 3 we give value relation to field and the field overposed inverse conclude in Section

Consider the Beltrami

in the complex plane exponent α . The Beltrami

by their sonic values. Thus throughout this paper by pressure, density, and speed we mean normalized pressure, normalized density, and normalized speed, respectively. For example, according to this convention $q_o^s = 1$ at sonic speed. (Here and below the superscript "s" has been used to denote the specified variables and the subscript "o" to denote the values of the specified variables on the profile only. Occasionally subscript "o" will not be used when its purpose is implicit from the context). Because the free stream Mach number is specified here independently of the speed distribution, the above problem of finding the airfoil which will have the modified C_p is overposed. Thus the interest in this overposed problem is due to aeronautical considerations.

The central idea of this paper is to work with the equations that have the least, preferably no, nonlinearity. For compressible fluid flow, the best we can do is to work with the equations derived in our earlier paper [1], where the nonlinearity has been shown to be very mild. It turns out to be the right approach for our purpose as shown in this paper. In that paper [1] we have reformulated the compressible fluid flow equations as the Beltrami equation and discussed the solution of the well-posed inverse problem using these equations. In this paper we make use of the Beltrami formulation of fluid flow to discuss three important issues related to the solution of the overposed inverse design problem. These issues are: (i) the mean value relation for the Beltrami equation which is a general result; (ii) the application of the mean value relation to find the compatibility condition between M_∞^s and q_o^s which answers the existence of solution to the overposed problem; and (iii) the application of the compatibility (or solvability) condition in reformulating the overposed problem as a wellposed problem without solving the fluid flow equations.

The rest of the paper is laid out as follows. In Section 2 we discuss the solution of the Beltrami equation and derive the mean value relation for this equation. Then in Section 3 we give some preliminaries on compressible flow and apply this mean value relation to obtain the compatibility condition: the relation between the far field and the field values on the body. In Section 4 we discuss the solution of the overposed inverse problem. In Section 5 we give some numerical results. Finally we conclude in Section 6.

2. THE BELTRAMI EQUATION

Consider the Beltrami equation

$$u_\sigma = f(\sigma) \quad (1)$$

in the complex plane $\Omega_\sigma: |\sigma| \leq 1$, where $f(\sigma)$ satisfies a Hölder condition with exponent α . The particular solution $u(\sigma)$ to this equation is given by [1, 6]

$$u(\sigma) = -\frac{1}{\pi} \iint_{\Omega_\sigma} \frac{f(\zeta)}{\zeta - \sigma} d\zeta d\eta, \quad (2)$$

where $\zeta = \xi + i\eta$. We first derive the mean value relation for the Beltrami equation which will be useful later for exposition.

2.1. The Mean Value Relation

For an arbitrary circle $\Omega_\sigma: |\sigma| \leq 1$ entirely contained in G and Hölder continuous $f(\sigma)$, every solution of the equation $u_\sigma = f(\sigma)$ regular in G satisfies the relation

$$u(\sigma = 0) = \frac{1}{2\pi} \int_0^{2\pi} u(x) dx - \frac{1}{\pi} \iint_{\Omega_\sigma} \frac{f(\zeta)}{\zeta} d\zeta d\eta, \quad (3)$$

where $u(x) = u(\sigma = e^{ix})$ and $f(\sigma)$ may have explicit nonlinear dependence on u and its derivatives.

Proof. From (1) and (2) it follows that the general solution to $u_\sigma = f(\sigma)$ is given by

$$u(\sigma) = -\frac{1}{\pi} \iint_{\Omega_\sigma} \frac{f(\zeta)}{\zeta - \sigma} d\zeta d\eta + g(\sigma), \quad (4)$$

where $g(\sigma)$ is an analytic function of σ . We assume that u and $g(\sigma)$ are regular in $|\sigma| \leq 1$. From (4) we have

$$u(\sigma = 0) = -\frac{1}{\pi} \iint_{\Omega_\sigma} \frac{f(\zeta)}{\zeta} d\zeta d\eta + g(\sigma = 0). \quad (5)$$

Here and below we use the notation $\sigma = 0$ for $\sigma = (0, 0)$. Since $g(\sigma)$ is regular, application of the mean value theorem for harmonic functions to Eq. (4) implies

$$g(\sigma = 0) = \frac{1}{2\pi} \int_0^{2\pi} u(x) dx + \frac{1}{\pi} \iint_{\Omega_\sigma} \left(\frac{1}{2\pi} \int_0^{2\pi} \frac{f(\zeta)}{\zeta - e^{ix}} dx \right) d\zeta d\eta. \quad (6)$$

It is an elementary exercise to show that the second integral in (6) vanishes and we have

$$g(\sigma = 0) = \frac{1}{2\pi} \int_0^{2\pi} u(x) dx. \quad (7)$$

From (5) and (7), Eq. (3) follows.

The relation (3) can easily be modified to account for any finite number of singularities on the unit circle $|\sigma| = 1$. In this case we regularize u by subtracting the singularities and then applying (3). If $u_a(\sigma)$ has all the singularities and we define $\tilde{u} = u - u_a$, then \tilde{u} satisfies (1). Hence from (3) it follows

$$\tilde{u}(\sigma = 0) = \frac{1}{2\pi} \int_0^{2\pi} \tilde{u}(x) dx - \frac{1}{\pi} \iint_{\Omega_\sigma} \frac{f(\zeta)}{\zeta} d\zeta d\eta. \quad (8)$$

Next we apply the mean value relations (3) and (8) to the compressible fluid flow equations.

3.1. P_f

Brie details a body

The va values. for sub

Here θ these e

in the and be χ depe functio

The is a ve Under are res; The the uni

In Eq. airfoil.

3.2. Th

Here values

From (

3. COMPRESSIBLE FLOWS

3.1. Preliminaries

Briefly, but briefly only, we review the basic equations of compressible flow. For details the reader should refer [1]. Our interest is in compressible fluid flow past a body. The potential equations of compressible fluid flow are [1, 7]

$$(3) \quad \nabla \cdot (\rho \mathbf{q}) = 0; \quad \nabla \times \mathbf{q} = 0; \quad p = \rho^\gamma. \quad (9)$$

The variables have their usual meaning and have been normalized by their sonic values. Thus at sonic speed $q = 1$, $p = 1$ and so on. The analogs of these equations for subsonic flows in the potential plane $w = \phi + i\psi$, are given by

$$(4) \quad \theta_\phi - K^{-1} v_\psi = 0, \quad \theta_\psi + K v_\phi = 0. \quad (10)$$

Here θ is the flow direction and K is a function of v . In [1], the author reduced these equations to the Beltrami equation

$$(5) \quad \tau_\sigma = f(\sigma) \quad (11)$$

in the complex plane $\Omega_\sigma: |\sigma| \leq 1$, where the mapping $\Omega_w \rightarrow \Omega_\sigma$ is conformal. Here and below $\tau = -v + i\theta$ is the complex velocity and $f(\sigma) = \chi \tau_\sigma$. The functions v and χ depend on Mach number "M." Occasionally we refer v as speed since v is a function of speed [1, 7].

The mapping $\Omega_w \rightarrow \Omega_\sigma$ allows the computation of $v(x)$ from specified $q(s)$ which is a very important aspect of this paper. This has been addressed before in [2]. Under this mapping, the images of the body and the infinity in the physical plane are respectively $|\sigma| = 1$ and $\sigma = (0, 0)$ in the circle plane.

The function τ has analytic singularities at the stagnation points, $\alpha = 0$, $\alpha = \alpha_s$ on the unit circle. For flows past an airfoil, τ is regularized by defining $\tilde{\tau} = \tilde{v} + i\tilde{\theta}$ as

$$(6) \quad \tilde{\tau} = \tau - \ln[(1 - \sigma)^{-\delta} (e^{i\alpha_s} - \sigma)^{-1}]. \quad (12)$$

In Eq. (12), the α_s is related to circulation and δ to the trailing edge angle of the airfoil.

3.2. The Far Field Constraint

Here we relate $\tau(\sigma = 0)$, the free stream values of τ , with $\tau(|\sigma| = 1)$, the surface values of τ . We apply the mean value relation (8) to (11). Then we have

$$(8) \quad \tilde{\tau}(\sigma = 0) = \frac{1}{2\pi} \int_0^{2\pi} \tilde{\tau}(x) d\alpha - \frac{1}{\pi} \iint_{\Omega_\sigma} \frac{f(\zeta)}{\zeta} d\zeta d\eta. \quad (13)$$

From (12) we have

$$(9) \quad \tilde{\tau}(\sigma = 0) = -v_x + i(\theta_x + \alpha_s), \quad (14)$$

where subscript ∞ refers to the values at infinity in the physical plane. The real and imaginary parts of (13) give

$$-v_\infty = \frac{1}{2\pi} \int_0^{2\pi} \tilde{v}(\alpha) d\alpha - \frac{1}{\pi} \text{Real} \left(\iint_{\Omega_\sigma} \frac{f(\zeta)}{\zeta} d\xi d\eta \right) \tag{15}$$

and

$$\theta_\infty = \frac{1}{2\pi} \int_0^{2\pi} \tilde{\theta}(\alpha) d\alpha - \frac{1}{\pi} \text{Imag} \left(\iint_{\Omega_\sigma} \frac{f(\zeta)}{\zeta} d\xi d\eta \right) - \alpha_\infty. \tag{16}$$

Equation (15) is the exact solvability condition for inverse problems. Equations (15) and (16) reduce to the usual mean value relation for harmonic functions in the incompressible case where $f(\zeta) = 0$. These equations relate the surface values of the field variables θ and v (speed and Mach number are functions of v) to the corresponding free stream values. The area integral in (13) (or (15) and (16)) is due to the nonlinearities of compressible flows. The nonlinearities of compressible flow is also implicit in the mapping of the physical plane onto the circle plane via the potential plane [1, 2]. Due to these area integrals, the exact free stream values cannot be inferred a priori from the surface values.

3.3. Remarks Based on Numerical Experiments

Numerical evidence (see Section 5) strongly suggests that the contribution of the area integral in (13) is negligible for all practical purposes, i.e.,

$$\tilde{\tau}^a(\sigma = 0) \approx \tilde{\tau}(\sigma = 0),$$

where

$$\tilde{\tau}^a(\sigma = 0) = \frac{1}{2\pi} \int_0^{2\pi} \tilde{\tau}(\alpha) d\alpha. \tag{17}$$

Here and below the superscript "a" will refer to the approximate value in the above sense. The real part of (17) is (see Eq. (14))

$$-v_\infty^a = \frac{1}{2\pi} \int_0^{2\pi} \tilde{v}(\alpha) d\alpha. \tag{18}$$

This relation allows one to estimate M_∞^a , from $\tilde{v}(\alpha)$ without solving the equations of compressible fluid flow.

To be more precise, suppose M_∞ is the exact free stream Mach number which satisfies (15) and M_∞^a is the approximate value of M_∞ which satisfies (18) (obtained by neglecting the contribution from the area integral in (15)). Considerable numerical experiments on various airfoils suggest that

$$\Delta M_\infty = |M_\infty - M_\infty^a| < \varepsilon, \tag{19}$$

where
 nume
 exper
 quote
 Num
 fact t
 Nu
 $C_p(s)$
 distri
 $C_p^a(s)$
 to the
 will b
 also g
 tion a

4.1. T

For
 with t
 Eq. (1:
 nonlin
 priori.
 the co
 solvab
 M_∞^s to
 not sar
 in orde
 of $|M_\infty$
 efficien

We hav
 best est

where ε is of the order of 0.006 at worse. The numerical value 0.006 is obtained numerically and does not have a theoretical basis. However, extensive numerical experiments suggests that in most cases this figure is much smaller than the above quoted figure. (We had only one case where we encountered a figure close to 0.006.) Numerical evidence in support of this is given in Section 5. This is partly due to the fact that $f(\sigma)$ in Eq. (11) is $O(M^4)$ (see [1]).

Numerical evidence (19) implies the following for the pressure distribution: if $C_p(s)$ and $C_p^a(s)$ denote the pressure distributions obtained from the same speed distribution but with Mach numbers M_∞ and M_∞^a , respectively, then $C_p(s)$ and $C_p^a(s)$ will be even closer because the pressure distribution is inversely proportional to the square of the free stream Mach number to the leading order [5]. In fact they will be identical for all practical purposes. Numerical evidence in support of this is also given in Section 5. This will allow one to correct an arbitrary pressure distribution a priori which will have a solution for all practical purposes.

4. THE OVERPOSED INVERSE PROBLEM

4.1. The Approximate Solvability Condition

For a solution to exist, the specified data $\tilde{v}_0^s(\alpha)$ and M_∞^s have to be compatible with the solvability condition (15). However, these specified data may not satisfy Eq. (15) and thus the overposed inverse problem may not be solvable. Due to the nonlinear terms in (15), the exact solvability of this problem cannot be decided a priori. Usually the wellposed problem with $\tilde{v}_0^s(\alpha)$ as the only input is solved to find the corresponding free stream Mach number M_∞ . The $\tilde{v}_0^s(\alpha)$ and M_∞ satisfies exact solvability condition (15). The value of M_∞ is then compared with the specified M_∞^s to decide the approximate solvability of this overposed problem. If these are not same then the specified $\tilde{v}_0^s(\alpha)$ is to be modified through some rational procedure in order to impose the desired M_∞^s . In fact we can estimate a useful upper bound of $|M_\infty - M_\infty^s|$ without solving the well-posed problem. This will be the basis of the efficient numerical method discussed in the next section. We have

$$\begin{aligned}
 |M_\infty - M_\infty^s| &= |M_\infty - M_\infty^a + M_\infty^a - M_\infty^s| \\
 &\leq |M_\infty - M_\infty^a| + |M_\infty^a - M_\infty^s| \\
 &= \Delta M_\infty + \Delta M_\infty^s \\
 &\leq \varepsilon + \Delta M_\infty^s \\
 &= \varepsilon \quad \text{if } \Delta M_\infty^s = 0.
 \end{aligned}
 \tag{20}$$

We have used Eqs. (19) in (20) and the notation $\Delta M_\infty^s = |M_\infty^a - M_\infty^s|$. Thus the best estimate of this is ε if we have $\Delta M_\infty^s = 0$, i.e.,

$$\text{if } M_\infty^s = M_\infty^a \quad (21a)$$

$$\Rightarrow v_\infty^s = v_\infty^a \quad (21b)$$

$$\Rightarrow v_\infty^s = -\frac{1}{2\pi} \int_0^{2\pi} \tilde{v}(\alpha) d\alpha. \quad (22)$$

We have used (18) to arrive at (22) from (21b). It follows from (20) that the exact free stream Mach number M_∞ will be within $\pm \varepsilon$ of M_∞^s , if the speed distribution $\tilde{v} = \tilde{v}_o^s(\alpha)$ and M_∞^s is consistent with (22). Since ε is very small (see Eq. (19)), we consider this small error in M_∞ tolerable for all practical purposes. In fact our experience shows that the numerical error in computing M_∞ is of the order ε . Thus it is justified to take (22) as the solvability condition for all practical purposes.

If $\tilde{v}_o^s(\alpha)$ does not satisfy (22), then it is modified a priori to satisfy this constraint in the same spirit as in [3]. We briefly outline this modification procedure from [3].

4.2. Modification of the Speed Distribution

If $\tilde{v}_o^s(\alpha)$ does not satisfy (22), then \tilde{v}_o^s is modified to \tilde{v}_o , where

$$\tilde{v}_o = \tilde{v}_o^s + \gamma f(\alpha), \quad (23)$$

where $f(\alpha)$ is a suitable correction term. This can be chosen so that it is zero outside an interval (α_1, α_2) , leaving it the same outside (α_1, α_2) . Substituting (23) in (22) with $\tilde{v} = \tilde{v}_o$ gives

$$\gamma = b_1 / \frac{1}{2\pi} \int_0^{2\pi} f(\alpha) d\alpha, \quad (24)$$

where

$$b_1 = -v_\infty^s - \frac{1}{2\pi} \int_0^{2\pi} \tilde{v}_o^s(\alpha) d\alpha. \quad (25)$$

For our purpose we choose $f(\alpha)$ to be 1. Then Eq. (24) reduces to

$$\gamma = b_1. \quad (26)$$

We solve the well-posed problem with modified \tilde{v}_o as the input data as discussed in the next section.

4.3. Brief Description of the Numerical Method

First we briefly review the solution of the well-posed inverse problem from [1] to make the paper self-contained. The reader is referred to [1] for details. The $\tilde{v}_o^s(\alpha)$ can easily be computed from the specified $q_o^s(s)$ and vice versa (see [2]). An iterative method based on Eq. (13) yields $\tilde{\theta}(\alpha)$ which is used to generate the profile.

spe
str
an
spe
fre
i.e.
the
mo
pro
tio
 $\tilde{v}_o(\alpha)$

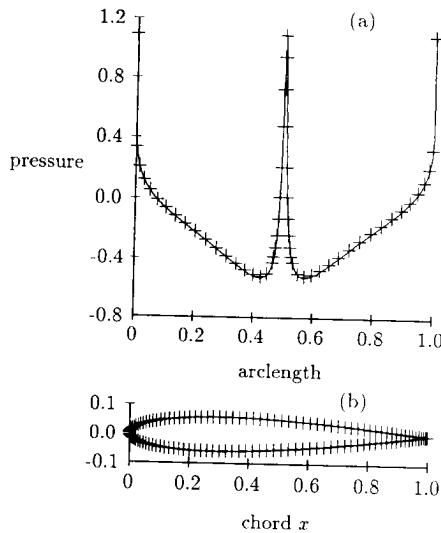
(i)
sol
sol

F
a p
corr

(21a) Now we address the overposed problem: generating a profile which has a
 (21b) specified pressure distribution $C_p(s)$. The speed distribution $q_o^s(s)$ and the free
 (22) stream Mach number M_∞^s are computed from $C_p(s)$ using the Bernoulli's relation
 and the ideal gas law [5]. Thus the problem is generating a profile which has a
 specified $q_o^s(s)$ at a given free stream Mach number M_∞^s . The $\tilde{v}_o^s(x)$ is computed
 from $q_o^s(s)$ (see [2]). We compute v_∞^a and hence M_∞^a using Eq. (18). If $M_\infty^a \neq M_\infty^s$,
 i.e., if $\tilde{v}_o^s(x)$ does not satisfy (22), then it is modified according to Section 4.2 and
 the corresponding $q_o(s)$ is also computed. The inverse problem is then solved with
 modified $\tilde{v}_o(x)$ as the input data by exactly the same procedure as in [1]. This
 provides the profile and the free stream Mach number M_∞ . The pressure distribu-
 tion $C_p(s)$ on the designed airfoil is computed from the $q_o(s)$, corresponding to
 $\tilde{v}_o(x)$, and M_∞ . Next we describe our numerical results.

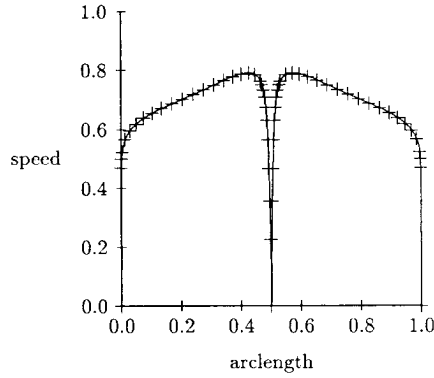
5. NUMERICAL RESULTS

In this section we present numerical results that exemplifies the following issues:
 (i) to justify the estimate in (19); (ii) to justify the effectiveness of the approximate
 solvability condition (22); (iii) to determine a priori the existence/nonexistence of
 solution to the overposed problem in an approximate sense (see Eq. (22)); and



(a) Input (---) and modified (+ +) pressure distributions. (b) Exact (---) and designed (+ +) airfoils.

FIG. 1. Compares the input pressure distribution with the modified pressure distribution (corrected a priori). Compares the airfoil corresponding to the modified speed distribution with the airfoil corresponding to the original speed distribution (see Fig. 2).

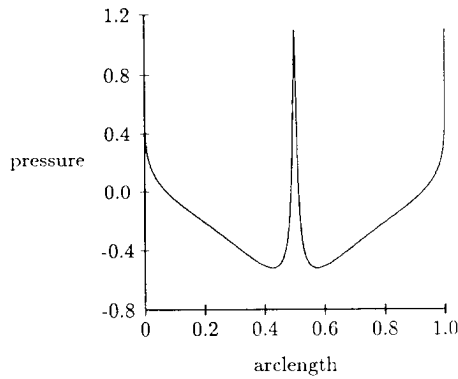


Input (—) and modified (+ +) speed distributions.

FIG. 2. Comparison of the input speed distribution with the modified speed distribution (which satisfies approximate solvability condition (18)).

(iv) to solve the overposed problem by imposing the specified M_∞^s . We discuss each of these issues in the same order as listed above. We have drawn the inference by carrying out the following numerical experiments on various airfoils at various conditions. We, however, report only a few cases for the sake of brevity and clarity.

First we justify the estimate (19). Input Euler pressure distribution C_p on Naca0012 airfoil is shown by the solid curve in Fig. 1. This corresponds to the speed distribution $q_o^s(s)$ at $M_\infty = 0.6$ as shown by the solid curve in Fig. 2 and, hence, these data are compatible. We compute $M_\infty^a = 0.6006$ from $q_o^s(s)$ by



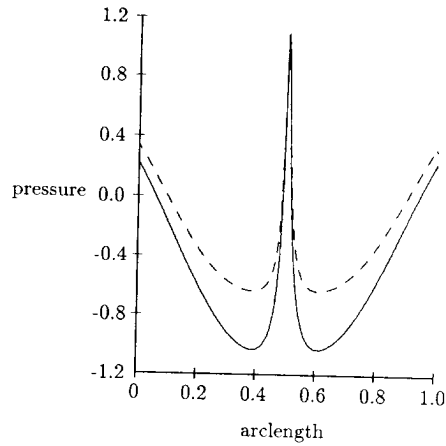
Design (—) and modified (- -) pressure distributions.

FIG. 3. Comparison of the design pressure distribution over the designed airfoil at $M_\infty = 0.6035$ with the modified pressure distribution (a priori) of Fig. 1a. Notice the accuracy in the figure (they are virtually same).

FIG.

the me
 $|M_\infty - M_\infty^a|$
 Next
 practical
 tribution
 speed di
 modifyin
 modified
 the mod
 that the

FIG.

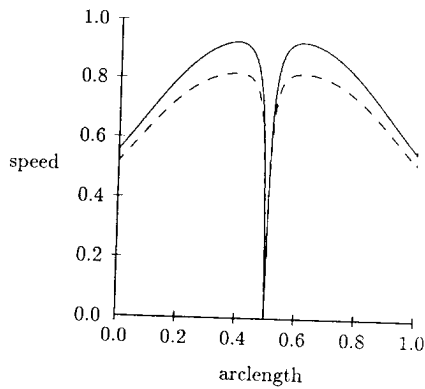


Target (—) and design (+ +) pressure distributions.

FIG. 4. Comparison of the target pressure distribution with the design pressure distribution.

the method outlined in Section 4.3. We find that the difference $\Delta M_\infty = |M_\infty - M_\infty^a| = 0.0006$ satisfies (19).

Next we show that the approximate solvability condition (22) is exact for all practical purposes. For this purpose we need to show that the modified speed distribution which satisfies the approximate solvability condition (22) and the exact speed distribution are same for all practical purposes. We impose $M_\infty^a = 0.60$ by modifying the $\tilde{v}_o(x)$ by the method of Section 4.2. We compute $q_o(x)$ from the modified $\tilde{v}_o(x)$ and $q_o(s)$ from $q_o(x)$. In Fig. 2 we compare the original, $q_o^*(s)$, and the modified, $q_o(s)$, speed distributions. The agreement is excellent which shows that the contribution of the double integral in (15) is indeed negligibly small. This



Target (—) and modified (+ +) speed distributions.

FIG. 5. Comparison of the target speed distribution with the modified speed distribution.

confirms that the approximate solvability condition is excellent for all practical purposes. This is further confirmed by the remarkable agreement between the modified pressure distribution (based on the modified speed distribution $q_o(s)$ and $M_\infty = 0.6$) and the exact pressure distribution in Fig. 1a.

Next we design the airfoil from the modified speed and compare it against original Naca0012 airfoil in Fig. 1b. Again we find that the agreement is excellent. In our design process, we recover the free stream Mach number to be 0.6002 which is close to 0.6. Thus we have been able to impose the free stream Mach number within an error 0.0002 which is presumably tolerable for all practical purposes. In Fig. 3 we find excellent agreement between the pressure distribution at $M_\infty = 0.6002$ on the designed airfoil and the modified pressure distribution which was calculated a priori. This establishes that we can correct any arbitrary pressure distribution a priori within an error which is acceptable for all practical purposes.

Next we take an arbitrary pressure distribution which is shown in Fig. 4. From Bernoulli's relation and gas law, we have $M_\infty^s = 0.60$ and speed distributions $q_o^s(s)$ of Fig. 5. These data may not be compatible and thus there may be no profile having the C_p of Fig. 4. In fact the free stream Mach number associated with $q_o(s)$ of Fig. 5 is 0.66. We intend to modify the speed distribution as little as we can so that it has a solution (airfoil) with $M_\infty \approx M_\infty^s = 0.60$. In order to impose $M_\infty = 0.60$ approximately, we modify the speed distribution according to Eq. (18) which is also shown in Fig. 5. The inverse solution to this well-posed problem with the modified speed as input data produces the airfoil shown in Fig. 6 and the free stream Mach number 0.6035 which is close enough to 0.60. Thus we have achieved a solution of

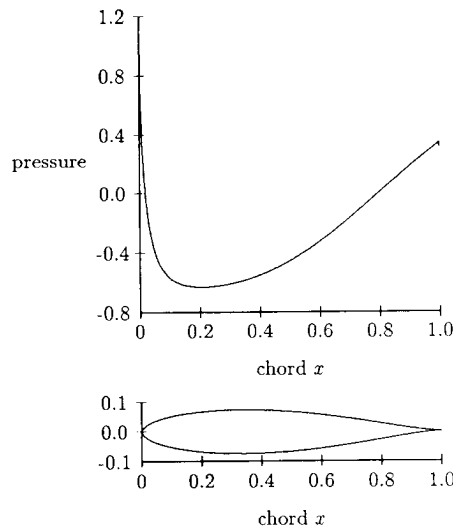
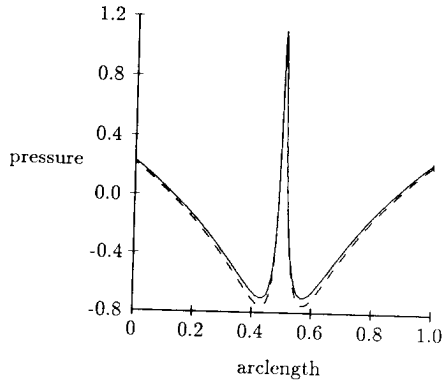


FIG. 6. The designed airfoil and the design pressure distribution along the chord from the modified speed distribution of Fig. 8.

FIG

the ov
Fig. 6
with
regard
prescr
not cl
input
In
Berno
shown
at pos

F

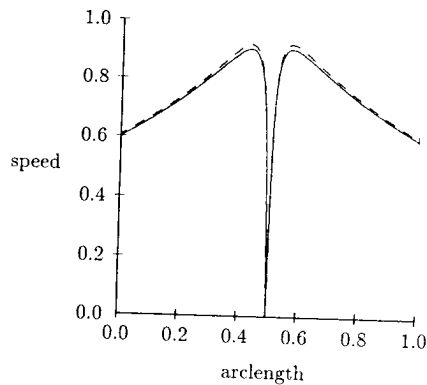


Target (—) and design (- - -) pressure distributions.

FIG. 7. Comparison of the target pressure distribution with the design pressure distribution.

the overposed problem successfully by modifying the speed distribution a priori. In Fig. 6 we also show the design pressure distribution and in Fig. 4 we compare it with the input pressure distribution. A few comments should be made here regarding this computation. We see in Figs. 4 and 5 that the modified and the prescribed speed and pressure distributions is compatible with $M_x = 0.66$ which is not close to the desired value $M_x = 0.60$. If these were close, then the modified and input distributions will also be very close as seen in the next example.

In Fig. 7 we show yet another arbitrary (target) pressure distribution. From Bernoulli's relation and gas law, we find $M_x^s = 0.60$ and speed distributions $q_o^s(s)$ shown in Fig. 8. We intend to modify the pressure and speed distributions as little as possible so that it has a solution (airfoil) with $M_x \approx M_x^s = 0.65$. We impose



Target (—) and modified (+ +) speed distributions.

FIG. 8. Comparison of the target speed distribution with the modified speed distribution.

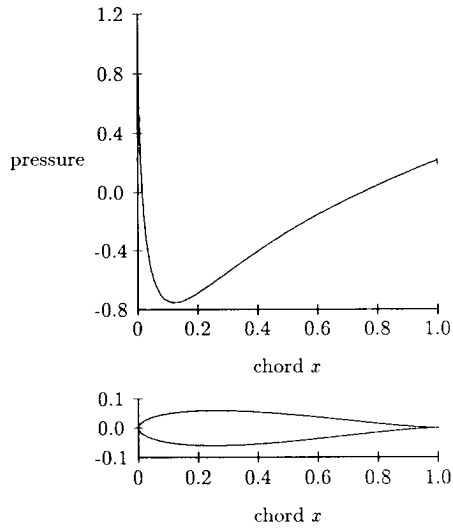
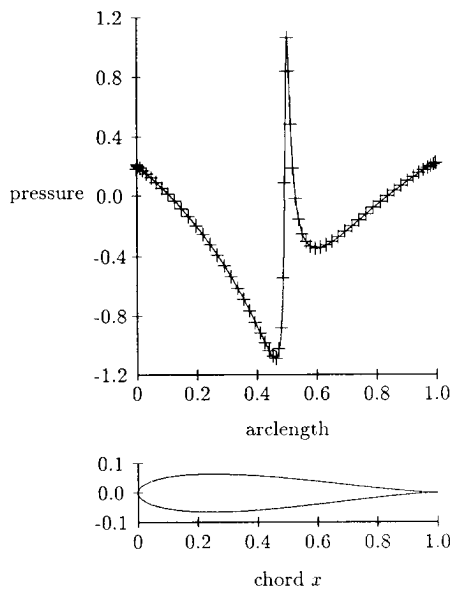


FIG. 9. The designed airfoil and the design pressure distribution along the chord from the modified speed distribution of Fig. 8.



Input (—) and modified (+ +) pressure distributions.

FIG. 10. Comparison of the Euler pressure distribution with the modified pressure distribution (corrected a priori). The Euler pressure distribution is over 6% thick Kutta airfoil at $M_\infty = 0.5$ and angle of attack = 2° .

M_∞
 which
 inve
 shov
 Mac
 of th
 In F
 tribu
 pres
 the
 to th
 In
 pres
 Mac
 distr
 0.5
 mod
 Mor

In
 and
 to ir
 tribu
 have

Th

1. P.
2. P.
3. P.
4. F.
- Ne
5. H.
- p.
6. R.
- Ne
7. L.
- p.

$M_\infty = 0.65$ approximately by modifying the speed distribution according to Eq. (18) which is also shown in Fig. 8. With the modified speed as input data, we solve the inverse problem. This generates the airfoil and associated pressure distribution shown in Fig. 9. Also as part of the solution we obtain the associated free stream Mach number to be 0.656 which is close to 0.65. Thus we have achieved a solution of the overposed problem successfully by modifying the speed distribution a priori. In Fig. 7 we compare the design pressure distribution with the input pressure distribution. In Figs. 7 and 8 we see that the modified and the prescribed speed and pressure distributions are very close, as one would probably like. This is because the input speed distribution is exactly compatible with $M_\infty = 0.648$ which is close to the desired value $M_\infty = 0.65$.

In Fig. 10 we show a case with lift. The solid curve in Fig. 10 shows the Euler pressure distribution on 6% thick kutta airfoil at 2° angle of attack and free stream Mach number of 0.5. Here again we compute the M_∞^a from the associated speed distribution by the method outlined in Section 4.3. We find M_∞^a to be accurate to 0.5 up to four decimal places. This supports the inequality (19). Therefore the modified pressure distribution practically remains identical as that seen in Fig. 10. More extensive numerical examples will be reported elsewhere.

6. CONCLUSION

In this paper we have addressed the issue of solvability of the overposed problem and discussed a method to modify any arbitrary speed distribution a priori in order to impose any arbitrary free stream Mach number. The corresponding pressure distribution is also predicted a priori, which is exact for all practical purposes. We have justified the efficiency of our approach through numerical computation.

ACKNOWLEDGMENT

This research in part has been supported by the NSF Grant DMS-8803669.

REFERENCES

1. P. DARIPA, *J. Comput. Phys.*, to appear.
2. P. DARIPA, *Q. Appl. Math.* **46**, No. 3, 505 (1988).
3. P. DARIPA AND L. SIROVICH, *J. Comput. Phys.* **63**, 311 (1986).
4. F. BAUER, P. R. GARABEDIAN, AND D. KORN, *Supercritical Wing Sections III* (Springer-Verlag, New York/Berlin, 1977), p. 296.
5. H. W. LIEPMANN AND A. ROSHKO, *Elements of Gas Dynamics* (Wiley Interscience, New York, 1957), p. 439.
6. R. COURANT AND D. HILBERT, *Methods of Mathematical Physics, Vol. II* (Wiley Interscience, New York, 1961), p. 830.
7. L. BERS, *Mathematical Aspects of Subsonic and Transonic Gas Dynamics* (Wiley, New York, 1958), p. 164.